Ultrahigh-Capacity and Long-Life Lithium–Metal Batteries Enabled by Engineering Carbon Nanofiber–Stabilized Graphene Aerogel Film Host

Changtai Zhao, Chang Yu,* Shaofeng Li, Wei Guo, Yang Zhao, Qiang Dong, Xiaoting Lin, Zhongxin Song, Xinyi Tan, Changhong Wang, Matthew Zheng, Xueliang Sun,* and Jieshan Qiu*

A safe, high-capacity, and long-life Li metal anode is highly desired due to recent developments in high-energy-density Li–metal batteries. However, there are still rigorous challenges associated with the undesirable formation of Li dendrites, lack of suitable host materials, and unstable chemical interfaces. Herein, a carbon nanofiber-stabilized graphene aerogel film (G-CNF film), inspired by constructional engineering, is constructed. As the host material for Li deposition, the G-CNF film features a large surface area, porous structure, and a robust skeleton that can render low local current density. This allows for dendrite-free Li deposition and mitigation of problems associated with large volume change. Importantly, the G-CNF film can keep high Li plating/stripping efficiency at nearly 99% for over 700 h with an areal capacity of 10 mA h cm^{-2} (the specific capacity up to 2588 mA h g^{-1} based on the total mass of carbon host and Li metal). The symmetric cells can stably run for more than 1000 h with low voltage hysteresis. The full cell with the LiFePO$_4$ cathode also delivers enhanced capacity and lowered overpotential. As two-in-one host materials for both cathodes and anodes in Li–O$_2$ batteries, the battery exhibits a capacity of 1.2 mA h cm^{-2}.

1. Introduction

Due to the high theoretical specific capacity (3860 mA h g^{-1}) and the lowest reduction potential (−3.04 V vs standard hydrogen electrode) of metallic lithium (Li), Li–metal batteries (LMBs), such as Li–S and Li–O$_2$ batteries, hold great promise as next-generation electrochemical energy storage devices

beyond the state-of-the-art Li-ion batteries. The applications include electric vehicles, grid storage, and all other fields with the requirement of high energy density.[1] In the past decade, considerable efforts have long been devoted to develop novel and advanced cathodes (sulfur and oxygen cathodes) that can cooperate with a Li metal anode to form a high-energy-density device.[2] Fortunately, significantly improved configuration and efficacy of host materials on cathodes have been achieved in recent years.[3] However, a severe and crucial problem of dendritic Li formation in Li anode was concealed, which can lead to low Coulombic efficiency and serious safety hazards during the repeating charge/discharge processes.[4] Low Coulombic efficiency, associated with continuous side reactions between dendritic Li and liquid electrolyte, as well as the formation of unstable solid electrolyte interphase (SEI),

further results in poor cycle performance of LMBs.[5] Under extreme circumstances, large Li dendrites may penetrate the separator and cause short circuits of battery, giving rise to thermal runaway, in particular for large devices.[6] Therefore, suppressing the formation of dendritic Li and stabilizing the SEI layer between metallic Li and the electrolyte are crucial in improving the cycle life and security capability of LMBs.[7] It is well-known that current density is one of the key factors to regulate the Li deposition behavior.[8] In general, Li dendrites are formed more easily under a large current density, which is inevitable for developing high-power-density batteries. Therefore, enabling a low local Li-ion flux and current density on the surface of the anode is an effective approach toward rendering uniform Li deposition without dendrite formation.[9] Moreover, according to the "hostless" nature of Li metal, the virtually infinite volume change is another large issue that impedes the practical applications of LMBs. An effective scaffold material is necessary and vital to reversibly store and strip Li, which is used to accommodate the dynamic volume change during charge/discharge processes, especially for a battery with a large areal capacity.[10]

Dr. C. Zhao, Prof. C. Yu, S. Li, W. Guo, Dr. Q. Dong, X. Tan, Prof. J. Qiu
State Key Lab of Fine Chemicals
Liaoning Key Lab for Energy Materials and Chemical Engineering
School of Chemical Engineering
Dalian University of Technology
Dalian 116024, China
E-mail: chang.yu@dlut.edu.cn; jqiu@dlut.edu.cn
Dr. C. Zhao, Y. Zhao, X. Lin, Z. Song, C. Wang, M. Zheng, Prof. X. Sun
Department of Mechanical and Materials Engineering
University of Western Ontario
London, ON N6A 5B9, Canada
E-mail: xsun9@uwo.ca

Based on the considerations above, 3D hosts, with low density, high surface area, large pore volume, robust skeleton, high conductivity, and chemical stability, are necessary for addressing the issues previously discussed.[11] Recent efforts in this direction have proven efficacious to a certain extent for mitigating dendritic Li growth and improving the electrochemical performance.[12] However, these efforts have generally reported a low limited areal capacity ($\leqq 2$ mA h cm^{-2}), which is lower than that of the required areal capacity ($\geqq 3$ mA h cm^{-2}) for practical applications.[13] Moreover, some of the recent reports have required a Cu foil as the current collector and some porous metals in the fabrication process, which results in a significantly higher density than that of Li (0.53 g cm^{-3}).[11c,14] This increases the weight percentage of inactive materials and drastically decreases the energy density of batteries. In addition, when the batteries are operated with a large capacity, dendritic Li is easily formed, even at a low current density.[7b] Thus, rationally configuring the advanced host materials with high conductivity, chemical stability, light density, and porous and freestanding structure is sought-after and crucial for rendering high-efficiency and long-life LMBs with high areal capacity.

Herein, we engineered a carbon-based host of carbon nanofiber–stabilized graphene aerogel film (G-CNF film) via a facile scalable strategy inspired by constructional engineering. The as-made G-CNF film features large surface area, porous structure, and a robust skeleton. As the host material for Li deposition, the G-CNF film can result in low local current density and mitigate problems with large volume change, especially with a large areal capacity. It also exhibits no obvious Li dendrite formation and excellent electrochemical performance. Specifically, the as-made G-CNF film can keep high Coulombic efficiency of nearly 99% for more than 700 h with an ultrahigh limited capacity of 10 mA h cm^{-2}. In this case, the specific capacities are as high as 7850 and 2588 mA h g^{-1} based on the mass of the carbon host and the total mass of the carbon host and Li metal, respectively. The symmetric cells can stably run for more than 1000 h with low voltage hysteresis at a practical current density of 1 mA cm^{-2}. Furthermore, utilizing G-CNF film@Li with a LiFePO$_4$ cathode for a full cell, it enables enhanced specific capacity and lowered voltage hysteresis. The applicability as two-in-one host materials in Li–O$_2$ battery was also explored.

2. Results and Discussion

The resultant G-CNF film was synthesized by a facile blade coating strategy inspired by constructional engineering. A viscous mixed gel with graphene oxide (GO) and electrospun carbon nanofibers was prepared first. After uniform blade coating and facile hydroiodic acid reduction, a smooth hybrid hydrogel film was formed. The hybrid aerogel film was yielded after being freeze-dried. The present method will be also suitable for preparing the porous hybrid film with graphene and other components such as MoS$_2$ nanosheets, carbon nanotubes, etc.

The morphology and structure of the as-made G-CNF film was investigated by scanning electron microscopy (SEM) and transmission electron microscopy (TEM), and the typical images are shown in **Figure 1** and Figure S1 (Supporting Information). It can be seen that the G-CNF film features an open and interconnected porous structure (Figure 1a). The large holes can store massive amounts of metallic Li and accommodate the dynamic volume change, suggesting promising potential as a host material for Li metal anode with an ultralarge capacity. The magnified SEM images of Figure 1b,c show that the G-CNF films are made of 3D graphene sheets, cross-linked by carbon nanofibers. The carbon nanofibers in this system not only act as scaffolds for preventing the stack of graphene sheets, but also are responsible for strengthening the interior structure of the film. The cross-section SEM image indicates that the thickness of G-CNF film is about 800 µm (the inset in Figure 1a). From above, the as-made G-CNF film possesses both the porous feature of an aerogel and the structure of a film. For comparison, graphene (G) film was also prepared in the same way, but without the carbon nanofibers. As shown in Figure 1d, the G film is also porous, but graphene sheets are aggregated to some degree. This decreases the effective pore volume for storing metallic Li and increases the difficulty of plating metallic Li inside the electrode. TEM images shown in Figure S1 (Supporting Information) further verify these topical morphologies. In addition, the composition and structural characteristics of G-CNF film were also investigated by X-ray diffraction (XRD) and Raman spectroscopy, and the results are shown in Figure S2 (Supporting Information). The XRD characteristic peaks of carbon and D- and G-band peaks in Raman spectra confirm the hybrid of graphene and carbon nanofibers.

As the host materials, these integrated characteristics of the as-made G-CNF film will be beneficial for LMBs with a large capacity. The metallic Li deposition behaviors on various host materials were investigated by SEM, and the results are shown in **Figure 2** and Figure S3 (Supporting Information). The G-CNF film was first subjected to the lithiation process and the formed SEI layer was observed when the voltage decreased to 0 V. It is evident from Figure 2a that the G-CNF film is put on a protective clothing of SEI layer and the metallic Li begins to nucleate on the surface of G-CNF film.[15] With the increase of Li deposition, the metallic Li was uniformly plated on the surface of graphene and CNF, evidenced by the increased thickness of graphene sheets. This can also be verified by the morphology change after being exposed under the electron beam for a period of time (Figure S4, Supporting Information). Interestingly, when the areal capacity of plated Li metal was increased to the standard (3 mA h cm^{-2}) of practical applications, there was no obvious Li dendrite formation (Figure 2c,d and Figure S3a (Supporting Information)). And, a clear information that some large pores are still present can be observed from the SEM image of the G-CNF film after discharging to 3 mA h cm^{-2}. This means that the pore volume is enough for storing more Li metal and alleviating the volume change during Li deposition. In the subsequent stripping process, the Li metal was observed to nearly disappear (Figure 2e). Similarly, the G film electrode also exhibited the dendrite-free behavior due to the relatively large surface area (Figure S3b, Supporting Information). In sharp contrast, the Cu foil showed obvious Li dendrite formation. This highlights the advantage of utilizing high-surface-area materials for achieving low local current and enabling the regulation of Li deposition. The metallic

ADVANCED
SCIENCE NEWS
www.advancedsciencenews.com

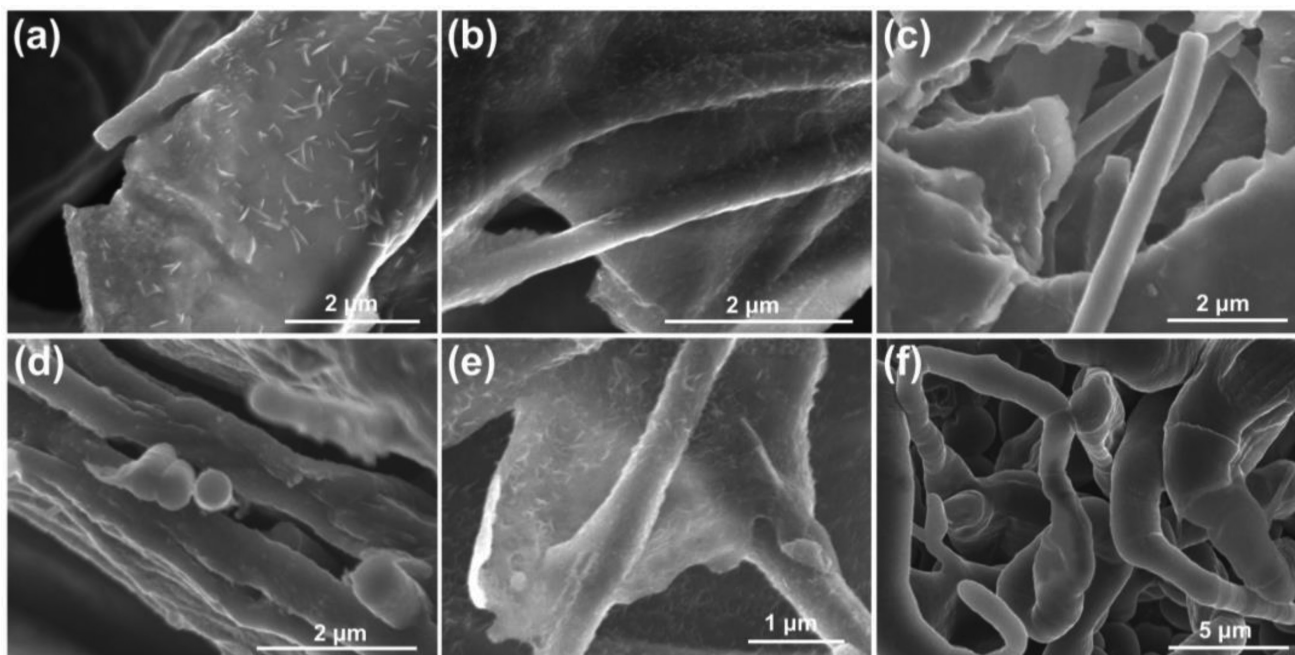NANO · MICRO
small
www.small-journal.com
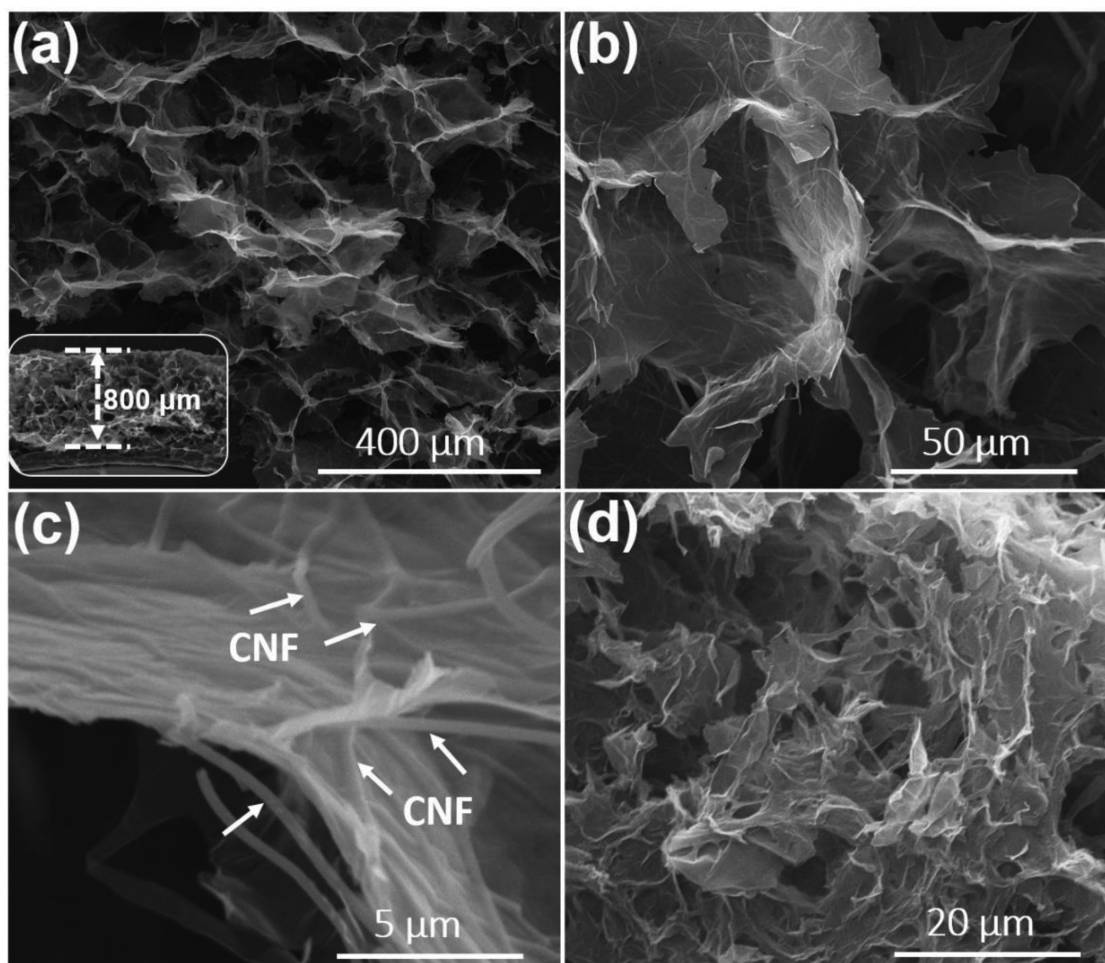
Figure 1. SEM images of the a–c) G-CNF film and d) G film.

Li deposition behaviors on G-CNF film were further investigated by examining the G-CNF film electrode after 50 cycles at a current density of 1 mA cm^{-2} with a limited capacity of 1 mA h cm^{-2}. As shown in Figure S5 (Supporting Information), the G-CNF film still shows dendrite-free and porous feature.

As the goal is to enable practical applications through high energy density, it is desirable and demanded to develop Li metal anodes with a high areal capacity and high specific capacity. But when batteries are operated with a large areal capacity, dendritic Li will be formed more easily, even at a low current density.[7b,16] So how to realize high-efficiency and high-capacity Li metal anode becomes more challenging and important. The as-made G-CNF film features a freestanding structure and can be directly used as the anode after being plated with Li metal, which will significantly enhance the specific capacity.

Based on the dendrite-free behavior of G-CNF film, the electrochemical performance was investigated via galvanostatic discharge/charge tests. Coulombic efficiency is one of the key parameters used to evaluate the Li metal deposition behavior and sustainability of a Li metal anode. It is defined as the ratio of Li stripped capacity to Li plated capacity in every cycle.[17] This was studied using a half-cell with Li metal as the counter electrode and the metal source. As shown in

Figure 3a, both G-CNF film and G film exhibited stable Coulombic efficiency over 170 cycles with a limited capacity of 1 mA h cm^{-2}. In contrast, Cu foil electrode showed a relatively stable but slightly lower Coulombic efficiency due to the more irreversible reaction of Li metal on the Cu foil electrode. When the limited capacity increased to 3 mA h cm^{-2} (Figure 3d), the Cu foil was only able to stably sustain 50 cycles, resulting in a lower Coulombic efficiency than G-CNF film and G film. G-CNF film and G film are also stable and keep the average Coulombic efficiency of nearly 98.5%. Notably, with an ultralarge limited capacity of 10 mA h cm^{-2}, Cu foil electrode exhibited fluctuating and low Coulombic efficiency (Figure 3d and Figure S6 (Supporting Information)). Under the same conditions, the G film electrode also showed rapid Coulombic efficiency decay in fewer than 30 cycles. In sharp contrast, the as-made G-CNF film was able to keep high plating/stripping efficiency of nearly 99% for more than 700 h. Figure 3e shows the stable plating/stripping behavior with small voltage hysteresis exhibited by the G-CNF film. Based on such a large areal capacity, the specific capacity is as high as 7850 mA h g^{-1}, based on the mass of the carbon host. The specific capacity is up to 2588 mA h g^{-1}, based on the total mass of carbon host with plated Li metal.

ADVANCED
SCIENCE NEWS
www.advancedsciencenews.com

NANO · MICRO
small
www.small-journal.com

Figure 2. SEM images of the G-CNF film after discharging to a) the voltage of 0 V, b) the capacities of 1 mA h cm^{-2} and c,d) 3 mA h cm^{-2}, e) discharging to the capacity of 3 mA h cm^{-2} and recharging to the voltage of 1.5 V, and f) the Cu foil after discharging to the capacity of 3 mA h cm^{-2}.

The high and stable Coulombic efficiency of the G-CNF film electrode even at a large areal capacity is attributed to the high specific surface area, which enables the ability to achieve low local current density, regulates the uniform deposition of Li metal, and promotes the formation of a stable and protective SEI layer.[18] The composition of the SEI layer in the G-CNF film was investigated by X-ray photoelectron spectroscopy (XPS), and

the results are shown in Figure S7 (Supporting Information). It was found that the SEI layer consisted of inorganic and organic components such as LiF, LiN$_x$O$_y$, ROLi, ROCOOLi, etc.[19] The large and inhomogeneous Li-ion flux on the surface of the Cu foil induced the growth of Li dendrites, which leads to serious safety hazards and low Coulombic efficiency during charge/discharge cycles. With the progressive growth of Li dendrites, the
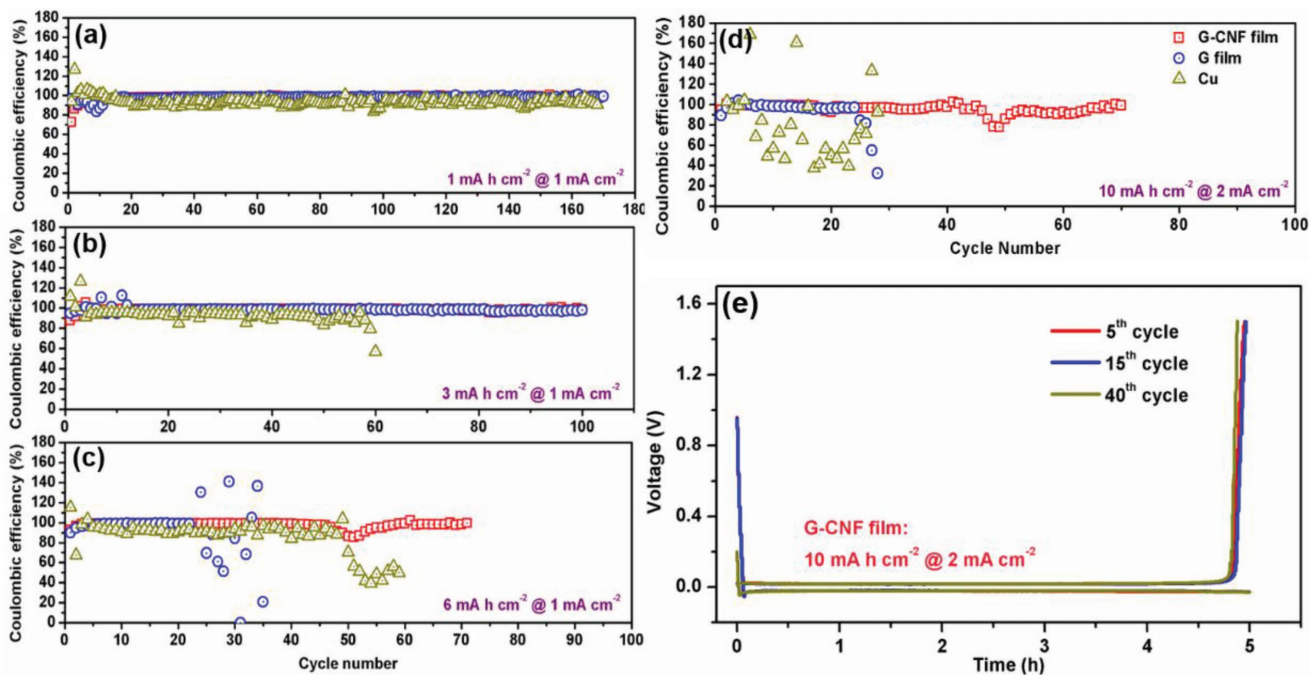

Figure 3. Coulombic efficiency of G-CNF film, G film, and Cu foil electrodes with different limited capacities of a) 1 mA h cm^{-2}, b) 3 mA h cm^{-2}, c) 6 mA h cm^{-2}, and d) 10 mA h cm^{-2}. e) The discharge/charge profiles of the G-CNF film with a limited capacity of 10 mA h cm^{-2}.

SEI layer underwent continuous regeneration, consuming large amounts of Li metal and electrolyte, ultimately resulting in a low Coulombic efficiency. Meanwhile, the formation of Li dendrites resulted in isolated Li particles ("dead Li"), inducing extra irreversible Li consumption.[20] The large fluctuation of Coulombic efficiency can be ascribed to the fracture of Li dendrites and the occasional reconnection of the fractured pieces.[21] These results demonstrate that designing porous, light, and robust 3D host materials may be a promising strategy to tackle the intrinsic problems of Li metal anodes and help reach the desired level of high energy density. Also, the use of scaffolds can help to minimize the volume fluctuation of electrodes.
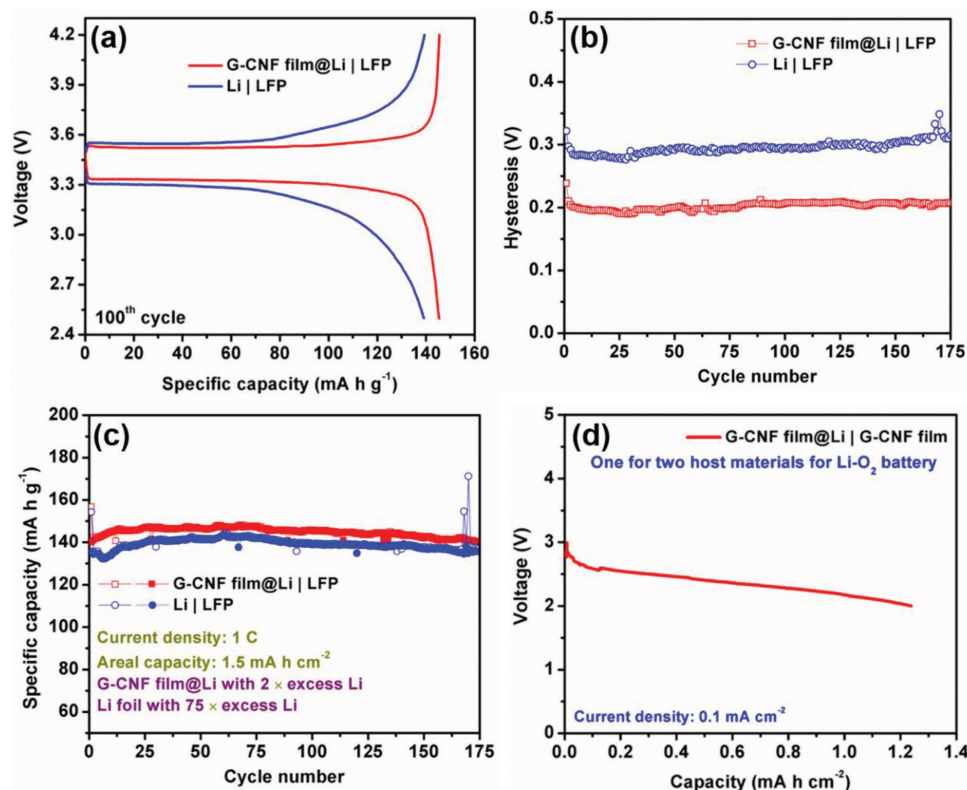
In order to further evaluate the long-term cycle performance, symmetric cells were tested with a limited capacity of 1 mA h cm^{-2} at a current density of 1 mA cm^{-2}. Before assembling the symmetric cells, 6 mA h cm^{-2} of Li metal was preplated into/onto the G-CNF film, G film, and Cu foil, which formed the G-CNF film@Li, G film@Li, and Cu foil@Li electrodes. As shown in **Figure 4**a, it is worth noticing that the G-CNF film@Li not only exhibited the lowest overpotential, but also significantly enhanced the cycle life up to 1000 h. The Cu foil@Li and bare Li electrodes showed markedly increased

overpotential after 500 h which originated from the accumulation of dead Li and SEI shell residue during the cycling process. As shown in Figure 4e, the small impedance of G-CNF film@Li symmetric cell also suggests uniform Li deposition.

In order to explore the application of the G-CNF film@Li, we constructed Li metal full cells by coupling the Li anodes with the lithium iron phosphate (LiFePO$_4$ and LFP in picture) cathode. The mass loading of LiFePO$_4$ is about 10 mg cm^{-2}, corresponding to about 1.5 mA h cm^{-2} of actual areal capacity. Before assembling the full cells, the G-CNF film@Li was prepared by preplating 3 mA h cm^{-2} of Li metal, corresponding to 2 excess Li. The full cells were tested at 1 C, and the results are shown in **Figure 5**. It can be noted that compared with the full cell using Li foil, the full cell with G-CNF film@Li anode exhibited lower overpotential in both the charge and discharge processes (Figure 5a and Figure S9 (Supporting Information)). The difference is more pronounced in Figure 5b. Additionally, the full cell with a G-CNF film@Li anode delivered an enhanced specific capacity, although 75 excess Li was used in the full cell with Li foil (Figure 5c). In order to further test the applicability of G-CNF film, the Li–O$_2$ battery was also built by using the G-CNF film as the two-in-one host materials in both the anode
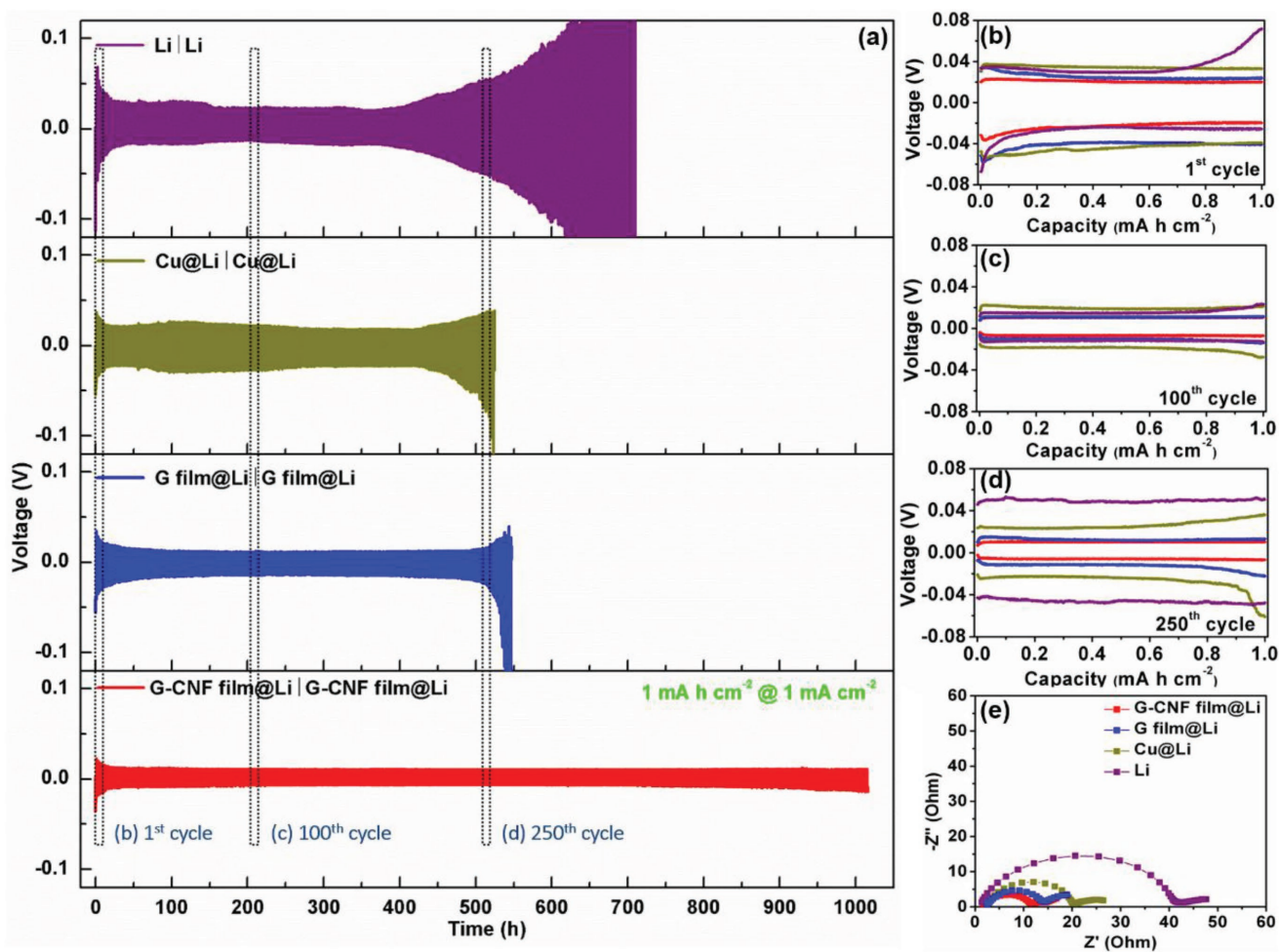
Figure 4. a) Cycle performance of various symmetric cells with a limited capacity of 1 mA h cm^{-2} at 1 mA cm^{-2}. The corresponding discharge/charge profiles at b) 1st cycle, c) 100th cycle, and d) 250th cycle. e) Nyquist plots of the various symmetric cells.

**ADVANCED
SCIENCE NEWS**

www.advancedsciencenews.com

NANO · MICRO

small

www.small-journal.com

Figure 5. a) Charge/discharge profiles of various full cells at the 100th cycle. b) Average voltage hysteresis and c) specific capacity of full cells at 1 C. d) Discharge profile of G-CNF film as two-in-one host materials for Li–O$_2$ battery.

and cathode. As shown in Figure 5d, the Li–O$_2$ battery delivered an areal capacity of 1.2 mA h cm^{-2}.

On the basis of the discussion above, the as-made G-CNF film demonstrated the effectiveness of a 3D host to regulate Li deposition and accommodate the dynamic volume change, resulting in an ultrahigh areal capacity and specific capacity. Through the full cell with LiFePO$_4$ and the Li–O$_2$ battery, the G-CNF film@Li demonstrated practicability and clear advantages over that of pure Li foil.

3. Conclusion

In summary, we have successfully engineered and constructed a carbon nanofiber–stabilized graphene aerogel film inspired by constructional engineering. The as-made composite not only possesses the porous nature of an aerogel but also inherits the structure of a film. As the host material for a Li anode, the film can effectively regulate the Li deposition in a uniform form and mitigate problems associated with the drastic volume change, especially with a large areal capacity. Based on the large areal capacity of 10 mA h cm^{-2}, the ultrahigh specific capacity of 2588 mA h g^{-1} was achieved based on the total mass of the carbon host and Li metal plated, and could be kept for over 700 h with a high Coulombic efficiency of nearly 99%. The symmetric cell based on G-CNF film@Li exhibited a long cycle life up to 1000 h with low voltage hysteresis. We expect that the present study can help inspire the

configuration of advanced host materials for safe and high-energy-density Li metal anodes.

4. Experimental Section

Synthesis of the G-CNF Film and G Film: GO nanosheets and carbon nanofibers were synthesized by a modified version of Hummer's method and electrospinning method, respectively, as reported in literature.[22] Typically, the GO dispersion was concentrated by centrifuging at 12 000 rpm several times. Carbon nanofibers were dispersed to solution by cutting and applying ultrasonic treatment. The dispersion was concentrated by centrifuging. Then, the two dispersions were mixed by vigorously stirring. A few drops of HCl solution (≈37 wt%) were added to further improve the viscosity of the mixed dispersion. After that, a hydrogel film was produced by casting the slurry on the glass. The as-made aerogel film was yielded after hydroiodic acid reduction and freeze-drying. G film was also prepared under the same conditions in the absence of carbon nanofibers.

Material Characterization: The as-made films were characterized by SEM (FEI NOVA NanoSEM 450), TEM (Tecnai G220), XRD (D/Max-III-type, Cu Kα X-ray source), Raman spectroscopy (HORIBA Scientific LabRAM HR), and XPS (Thermo ESCALAB 250).

Electrochemical Measurements: The as-made G-CNF film and G film could be used as the host materials without a current collector. The electrochemical performances of the as-made films were evaluated by assembling 2032-type coin cells. For the Coulombic efficiency test, the half-cells were built with the as-made sample or Cu foil as the work electrode and the Li metal as the counter electrode and Li metal source. 1 M lithium bis(trifluoromethanesulfonyl)-imide (LiTFSI) in 1,2-dimethoxyethane (DME)/1,3-dioxolane (DOL) (1:1 w/w) with 2 wt%

lithium nitrate ($LiNO_3$) was used as the electrolyte and Celgard 2400 was used as the separator. In order to form a stable SEI layer, the cells were run in the voltage window of 0–1.5 V at a current density of 0.2 mA cm^{-2} for 4 cycles. After that, the cells were discharged to a certain areal capacity and charged to 1.5 V. For the cycle performance test, the symmetrical cells were assembled by using a G-CNF film@Li (G film@Li and Cu@Li) electrode with 6 mA h cm^{-2} of preplated Li metal extracted from the half cell. These tests were performed on a Land battery test system. The electrochemical impedance spectroscopy (EIS) test was conducted on a Bio-Logic VSP electrochemical workstation at an open-circuit potential. The full cells were built by coupling the as-made Li anode (CNF film@Li, G film@Li, and Cu@Li) with 3 mA h cm^{-2} of preplated Li metal with a LiFePO$_4$ cathode. The mass loading of LiFePO$_4$ was about 10 mg cm^{-2}, corresponding to about 1.5 mA h cm^{-2} of actual area capacity. The as-made Li anode used in full cells was prestored 2 excess Li metal. The areal mass of G-CNF film was ≈1.27 mg cm^{-2}.

Supporting Information

Supporting Information is available from the Wiley Online Library or from the author.

Conflict of Interest

The authors declare no conflict of interest.

[1] a) M. D. Tikekar, S. Choudhury, Z. Tu, L. A. Archer, *Nat. Energy* **2016**, *1*, 16114; b) J. Zheng, M. H. Engelhard, D. Mei, S. Jiao, B. J. Polzin, J.-G. Zhang, W. Xu, *Nat. Energy* **2017**, *2*, 17012; c) C. Yang, L. Zhang, B. Liu, S. Xu, T. Hamann, D. McOwen, J. Dai, W. Luo, Y. Gong, E. D. Wachsman, L. Hu, *Proc. Natl. Acad. Sci. USA* **2018**, *115*, 3770; d) Q. Li, S. Tan, L. Li, Y. Lu, Y He, *Sci. Adv.* **2017**, *3*, e1701246.

[2] a) A. Manthiram, Y. Fu, Y.-S. Su, *Acc. Chem. Res.* **2013**, *46*, 1125; b) H.-J. Peng, J.-Q. Huang, X.-B. Cheng, Q. Zhang, *Adv. Energy Mater.* **2017**, *7*, 1700260; c) J. Lu, L. Li, J.-B. Park, Y.-K. Sun, F. Wu, K. Amine, *Chem. Rev.* **2014**, *114*, 5611; d) A. C. Luntz, B. D. McCloskey, *Chem. Rev.* **2014**, *114*, 11721; e) Y. Yang, G. Zheng, Y. Cui, *Chem. Soc. Rev.* **2013**, *42*, 3018; f) P. G. Bruce, S. A. Freunberger, L. J. Hardwick, J.-M. Tarascon, *Nat. Mater.* **2012**, *11*, 19.

[3] a) C. Zhao, C. Yu, S. Liu, J. Yang, X. Fan, H. Huang, J. Qiu, *Adv. Funct. Mater.* **2015**, *25*, 6913; b) C. Yu, C. Zhao, S. Liu, X. Fan,

J. Yang, M. Zhang, J. Qiu, *Chem. Commun.* **2015**, *51*, 13233; c) C. Zhao, C. Yu, M. Zhang, J. Yang, S. Liu, M. Li, X. Han, Y. Dong, J. Qiu, *J. Mater. Chem. A* **2015**, *3*, 21842; d) C. Zhao, C. Yu, M. N. Banis, Q. Sun, M. Zhang, X. Li, Y. Liu, Y. Zhao, H. Huang, S. Li, X. Han, B. Xiao, Z. Song, R. Li, J. Qiu, X. Sun, *Nano Energy* **2017**, *34*, 399.

[4] a) Q. Pang, X. Liang, A. Shyamsunder, L. F. Nazar, *Joule* **2017**, *1*, 871; b) E. Cha, M. D. Patel, J. Park, J. Hwang, V. Prasad, K. Cho, W. Choi, *Nat. Nanotechnol.* **2018**, *13*, 337; c) J. M. Tarascon, M. Armand, *Nature* **2001**, *414*, 359.

[5] a) N.-W. Li, Y. Shi, Y.-X. Yin, X.-X. Zeng, J.-Y. Li, C.-J. Li, L.-J. Wan, R. Wen, Y.-G. Guo, *Angew. Chem., Int. Ed.* **2018**, *57*, 1505; b) E. Kazyak, K. N. Wood, N. P. Dasgupta, *Chem. Mater.* **2015**, *27*, 6457; c) J.-S. Kim, D. W. Kim, H. T. Jung, J. W. Choi, *Chem. Mater.* **2015**, *27*, 2780; d) F. Ding, W. Xu, G. L. Graff, J. Zhang, M. L. Sushko, X. Chen, Y. Shao, M. H. Engelhard, Z. Nie, J. Xiao, X. Liu, P. V. Sushko, J. Liu, J. G. Zhang, *J. Am. Chem. Soc.* **2013**, *135*, 4450; e) H. Duan, Y.-X. Yin, Y. Shi, P.-F. Wang, X.-D. Zhang, C.-P. Yang, J.-L. Shi, R. Wen, Y.-G. Guo, L.-J. Wan, *J. Am. Chem. Soc.* **2018**, *140*, 82.

[6] Y. Sun, G. Zheng, Z. W. Seh, N. Liu, S. Wang, J. Sun, H. R. Lee, Y. Cui, *Chem* **2016**, *1*, 287.

[7] a) A. C. Kozen, C.-F. Lin, A. J. Pearse, M. A. Schroeder, X. Han, L. Hu, S. B. Lee, G. W. Rubloff, M. Noked, *ACS Nano* **2015**, *9*, 5884; b) S. Li, M. Jiang, Y. Xie, H. Xu, J. Jia, J. Li, *Adv. Mater.* **2018**, *30*, 1706375.

[8] a) A. O. Raji, R. V. Salvatierra, N. D. Kim, X. Fan, Y. Li, G. A. L. Silva, J. Sha, J. M. Tour, *ACS Nano* **2017**, *11*, 6362; b) H. Zhao, D. Lei, Y.-B. He, Y. Yuan, Q. Yun, B. Ni, W. Lv, B. Li, Q.-H. Yang, F. Kang, J. Lu, *Adv. Energy Mater.* **2018**, *8*, 1800266.

[9] a) X.-B. Cheng, H.-J. Peng, J.-Q. Huang, R. Zhang, C.-Z. Zhao, Q. Zhang, *ACS Nano* **2015**, *9*, 6373; b) X. Ji, D.-Y. Liu, D. G. Prendiville, Y. Zhang, X. Liu, G. D. Stucky, *Nano Today* **2012**, *7*, 10.

[10] a) S. Liu, A. Wang, Q. Li, J. Wu, K. Chiou, J. Huang, J. Luo, *Joule* **2018**, *2*, 184; b) Y. Zhao, Q. Sun, X. Li, C. Wang, Y. Sun, K. R. Adair, R. Li, X. Sun, *Nano Energy* **2018**, *43*, 368; c) D. Lin, Y. Liu, Z. Liang, H.-W. Lee, J. Sun, H. Wang, K. Yan, J. Xie, Y. Cui, *Nat. Nanotechnol.* **2016**, *11*, 626; d) Z. Liang, D. Lin, J. Zhao, Z. Lu, Y. Liu, C. Liu, Y. Lu, H. Wang, K. Yan, X. Tao, Y. Cui, *Proc. Natl. Acad. Sci. USA* **2016**, *113*, 2862; e) D. Lin, J. Zhao, J. Sun, H. Yao, Y. Liu, K. Yan, Y. Cui, *Proc. Natl. Acad. Sci. USA* **2017**, *114*, 4613; f) D. Lin, Y. Liu, W. Chen, G. Zhou, K. Liu, B. Dunn, Y. Cui, *Nano Lett.* **2017**, *17*, 3731; g) Y. Liu, D. Lin, Z. Liang, J. Zhao, K. Yan, Y. Cui, *Nat. Commun.* **2016**, *7*, 10992.

[11] a) L. Fan, H. L. Zhuang, W. Zhang, Y. Fu, Z. Liao, Y. Lu, *Adv. Energy Mater.* **2018**, *8*, 1703360; b) H. Ye, S. Xin, Y.-X. Yin, Y.-G. Guo, *Adv. Energy Mater.* **2017**, *7*, 1700530; c) S.-S. Chi, Y. Liu, W.-L. Song, L.-Z. Fan, Q. Zhang, *Adv. Funct. Mater.* **2017**, *27*, 1700348; d) Q. Song, H. Yan, K. Liu, K. Xie, W. Li, W. Gai, G. Chen, H. Li, C. Shen, Q. Fu, S. Zhang, L. Zhang, B. Wei, *Adv. Energy Mater.* **2018**, *8*, 1800564; e) N. Li, W. Wei, K. Xie, J. Tan, L. Zhang, X. Luo, K. Yuan, Q. Song, H. Li, C. Shen, E. Ryan, L. Liu, B. Wei, *Nano Lett.* **2018**, *18*, 2067; f) D. Lin, Y. Liu, A. Pei, Y. Cui, *Nano Res.* **2017**, *10*, 4003.

[12] a) C. Jin, O. Sheng, J. Luo, H. Yuan, C. Fang, W. Zhang, H. Huang, Y. Gan, Y. Xia, C. Liang, J. Zhang, X. Tao, *Nano Energy* **2017**, *37*, 177; b) R. Mukherjee, A. V. Thomas, D. Datta, E. Singh, J. Li, O. Eksik, V. B. Shenoy, N. Koratkar, *Nat. Commun.* **2014**, *5*, 3710.

[13] a) C. Yang, Y. Yao, S. He, H. Xie, E. Hitz, L. Hu, *Adv. Mater.* **2017**, *29*, 1702714; b) S. Matsuda, Y. Kubo, K. Uosaki, S. Nakanishi, *Carbon* **2017**, *119*, 119; c) A. Zhang, X. Fang, C. Shen, Y. Liu, C. Zhou, *Nano Res.* **2016**, *9*, 3428; d) G. Zheng, S. W. Lee, Z. Liang, H.-W. Lee, K. Yan, H. Yao, H. Wang, W. Li, S. Chu, Y. Cui, *Nat. Nanotechnol.* **2014**, *9*, 618.

ADVANCED
SCIENCE NEWS

www.advancedsciencenews.com

NANO · MICRO
small
www.small-journal.com

[14] a) Q. Yun, Y. B. He, W. Lv, Y. Zhao, B. Li, F. Kang, Q. H. Yang, *Adv. Mater.* **2016**, *28*, 6932; b) Q. Li, S. Zhu, Y. Lu, *Adv. Funct. Mater.* **2017**, *27*, 1606422; c) C.-P. Yang, Y.-X. Yin, S.-F. Zhang, N.-W. Li, Y.-G. Guo, *Nat. Commun.* **2015**, *6*, 8058.

[15] L. Liu, Y.-X. Yin, J.-Y. Li, N.-W. Li, X.-X. Zeng, H. Ye, Y.-G. Guo, L.-J. Wan, *Joule* **2017**, *1*, 563.

[16] Y. Zhang, W. Luo, C. Wang, Y. Li, C. Chen, J. Song, J. Dai, E. M. Hitz, S. Xu, C. Yang, Y. Wang, L. Hu, *Proc. Natl. Acad. Sci. USA* **2017**, *114*, 3584.

[17] X.-B. Cheng, R. Zhang, C.-Z. Zhao, Q. Zhang, *Chem. Rev.* **2017**, *117*, 10403.

[18] R. Zhang, X.-B. Cheng, C.-Z. Zhao, H.-J. Peng, J.-L. Shi, J.-Q. Huang, J. Wang, F. Wei, Q. Zhang, *Adv. Mater.* **2016**, *28*, 2155.

[19] T.-T. Zuo, X.-W. Wu, C.-P. Yang, Y.-X. Yin, H. Ye, N.-W. Li, Y.-G. Guo, *Adv. Mater.* **2017**, *29*, 1700389.

[20] D. Lin, Y. Liu, Y. Cui, *Nat. Nanotechnol.* **2017**, *12*, 194.

[21] D. Wang, W. Zhang, W. Zheng, X. Cui, T. Rojo, Q. Zhang, *Adv. Sci.* **2017**, *4*, 1600168.

[22] a) C. Zhao, C. Yu, B. Qiu, S. Zhou, M. Zhang, H. Huang, B. Wang, J. Zhao, X. Sun, J. Qiu, *Adv. Mater.* **2018**, *30*, 1702486; b) C. Zhao, C. Yu, M. Zhang, Q. Sun, S. Li, M. N. Banis, X. Han, Q. Dong, J. Yang, G. Wang, X. Sun, J. Qiu, *Nano Energy* **2017**, *41*, 66.